Macromolecules

ARTICLE

pubs.acs.org/Macromolecules

Poly(acrylic acid-*b*-styrene) Amphiphilic Multiblock Copolymers as Building Blocks for the Assembly of Discrete Nanoparticles

Anna C. Greene, Jiahua Zhu, Darrin J. Pochan, Xinqiao Jia,* and Kristi L. Kiick*

Department of Materials Science and Engineering, University of Delaware, 201 DuPont Hall, Newark, Delaware 19716, United States, and Delaware Biotechnology Institute, 15 Innovation Way, Newark, Delaware 19711, United States

Supporting Information

ABSTRACT:

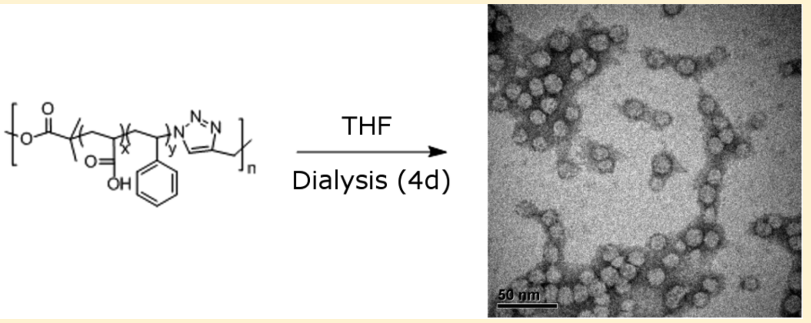

In order to expand the utility of current polymeric micellar systems, we have developed amphiphilic multiblock copolymers containing alternating blocks of poly(acrylic acid) and poly(styrene). Heterotelechelic poly(*tert*-butyl acrylate-*b*-styrene) diblock copolymers containing an α-alkyne and an ω-azide were synthesized by atom transfer radical polymerization (ATRP), allowing control over the molecular weight while maintaining narrow polydispersity indices. The multiblock copolymers were constructed by copper-catalyzed azide-alkyne cycloaddition of azide−alkyne end functional diblock copolymers which were then characterized by ^{1}H NMR, FT-IR and SEC. The *tert*-butyl moieties of the poly(*tert*-butyl acrylate-*b*-styrene) multiblock copolymers were easily removed to form the poly(acrylic acid-*b*-styrene) multiblock copolymer ((PAA−PS)$_9$), which contained up to 9 diblock repeats. The amphiphilic multiblock (PAA−PS)$_9$ (M_n = 73.3 kg/mol) was self-assembled by dissolution into tetrahydrofuran and extensive dialysis against deionized water for 4 days. The critical micelle concentration (cmc) for (PAA−PS)$_9$ was determined by fluorescence spectroscopy using pyrene as a fluorescent probe and was found to be very low at 2×10^{-4} mg/mL. The (PAA−PS)$_9$ multiblock was also analyzed by dynamic light scattering (DLS) and transmission electron microscopy (TEM). The hydrodynamic diameter of the particles was found to be 11 nm. Discrete spherical particles were observed by TEM with an average particle diameter of 14 nm. The poly(acrylic acid) periphery of the spherical particles should allow for future conjugation of biomolecules.

INTRODUCTION

One of the most interesting properties of block copolymers is their ability to self-assemble into numerous morphologies with spatial control on the nanometer scale.[1−7] These self-assembled structures have many potential uses in nanotechnology including drug delivery and block copolymer lithography for microelectronics.[8,9] Self-assembled micellar structures have also been employed as multifunctional cross-linkers for the formation of elastomeric hydrogels.[10] As much attention as di- and triblock copolymers have garnered, relatively little has been reported regarding the synthesis and characterization of alternating multiblock copolymers. There are numerous advantages for developing $(AB)_n$ multiblock copolymers, and one of the most fascinating is the formation of unique structures through the self-assembly of the multiblocks, such as unimolecular micelles[11,12] and flowerlike multimolecular micelles.[13] Multiblocks serve as compatibilizers for immiscible polymer blends[14,15] and also display unique mechanical and elastic properties due to the alternating structure of the synthetic polymer blocks.[16,17]

Less attention has been devoted to the study of multiblocks than di- and triblock copolymers most likely due to their more involved syntheses. Alternating multiblock copolymers are generally made by three different strategies. One technique involves the sequential addition of alternating monomers in one pot.[18−20] This method is useful for forming fairly well-defined multiblocks but is experimentally challenging, and block contamination can occur by the previous monomer if conversion is not complete. Alternatively, alternating multiblock polymers can be made by the condensation of α,ω-telechelic polymers (or peptides).[16,21−31] This method is straightforward, but the molecular weight

Received: December 16, 2010
Revised: February 2, 2011
Published: March 04, 2011

distributions of the polymers are quite broad, and it can also be difficult to synthesize polymers of large molecular weights due to the burial of the reactive chain ends as the polymerization proceeds. Multiblock polymers can also be produced via the combination of condensation chemistry with free radical polymerization by utilizing polyinitiators. These linear, alternating polymer-initiator assemblies are used to initiate the polymerization of a monomer of interest, typically by controlled free radical polymerization.[13,32−37] This method allows for the formation of higher molecular weight multiblocks, but despite the use of controlled radical polymerization initiators within the multiblocks, the molecular weight distributions are still broadened due to the polydispersity of the macroinitiator itself.

The self-assembly of multiblocks depends heavily on a variety of factors: polymer block constituents, the molecular weight of the polymer blocks, the hydrophobicity/hydrophilicity of blocks, and the number of blocks, among others.[38] In the early 1990s, Halperin theoretically predicted the formation of unimolecular micelles and multimolecular strings of micelles from multiblock copolymers.[11] Experimental studies have more recently shown a broad range of structures obtained from assembly of multiblock copolymers. In a study of alternating multiblocks of poly(dimethylacrylamide) and poly(*N*-isopropylacrylamide) (PNIPAM), unimolecular flowerlike micelles were observed by dynamic light scattering (DLS) for copolymers containing larger blocks of both polymers, while multimolecular flowerlike micelles were formed when the multiblocks comprised smaller blocks of both polymers.[13] Hadjiantoniou et al. have observed, via DLS studies, the formation of flowerlike micelles from multiblocks of poly[(2-dimethylamino)ethyl methacrylate-*b*-methyl methacrylate].[18,19] Alternating multiblock copolymers of poly(ethylene glycol) (PEG) and poly(styrene) (PS) yield various morphologies as observed by transmission electron microscopy (TEM) depending on the size of the poly(styrene) block relative to the PEG block.[12] Morphologies such as large leaflike aggregates, rodlike aggregates, and large compound micelles were observed over a range of poly(styrene) block sizes.[12] For poly(methylphenylsilane)-*b*-PEG multiblock copolymers, a range of structures were observed by TEM including micellar fibers, vesicles, and, surprisingly, helical superstructures; the structures could be varied based on the water content of the polymer solution.[22] More recently, Du et al. observed by DLS and TEM the existence of micelles, micellar aggregates, and vesicles for assembled multiblocks of PNIPAM−P*t*BA−PNIPAM.[39]

The examples above represent the few studies that combine the synthesis of alternating multiblocks with their study by DLS and TEM. There is also a dearth of DLS and TEM data to corroborate the formation of well-defined, low-dispersity distributions of assembled multiblocks at relevant length scales (particles <100 nm) for biomedical applications.[40] In addition, many of the previously reported multiblocks do not comprise highly functional blocks to which biologically relevant molecules can be attached. In this report, we address these limitations and report the synthesis of high molecular weight multiblocks containing functionality within the polymer. We report the synthesis of poly(acrylic acid-*b*-styrene) (PAA−PS) alternating multiblocks and the corresponding DLS and TEM characterization showing these particles to be spherical in nature and less than 35 nm in diameter. Future studies will elucidate the attachment of biomolecules and their potential presentation around the corona of these assembled multiblock particles for the purposes of drug delivery.

EXPERIMENTAL SECTION

Materials. All reagents were used without further purification unless specified. 3-(Trimethylsilyl)propargyl alcohol, 2-hydroxyethyl acrylate, 2-methyl-2-bromopropionyl bromide, copper(I) bromide (98%), *N*-(3-(dimethylamino)propyl)-*N*′-ethylcarbodiimide (EDC), *N*,*N*,*N*′,*N*′,*N*″-pentamethyldiethylenetriamine (PMDETA), tetra-*n*-butylammonium fluoride (TBAF), sodium azide, *tert*-butyl acrylate, trifluoroacetic acid (TFA), and styrene were purchased from Sigma-Aldrich or Fisher Scientific. Monomers were passed over a column of basic alumina to remove inhibitors prior to use. Deionized water was obtained through a NANOpure Diamond water purification system (Barnstead, Thermo Scientific).

Instrumentation. ^{1}H NMR spectra were recorded on a Bruker AV400 spectrometer using $CDCl_3$ or d_6-DMSO as a solvent containing 1% TMS as an internal reference. Size exclusion chromatography (SEC) was carried out using THF as the mobile phase at a flow rate of 1.0 mL/min on two Waters Styragel columns heated at 30 °C and a Waters 2414 refractive index detector. Data were analyzed using the Waters Empower software by comparison to a calibration curve of narrow polystyrene standards. FT-IR spectra were obtained on a Thermo Nicolet Nexus 670 spectrometer containing a DuraSamplIR II ATR accessory (SensIR Technologies). The polymeric sample was drop-cast from a THF solution onto the silicon ATR crystal and allowed to dry before data acquisition. The spectra were acquired at a resolution of 4 cm^{-1} from 550 to 4000 cm^{-1} with 128 average scans, and the data were processed with OMNIC software. A background scan of the bare silicon crystal was subtracted from all sample spectra. Fluorescence spectra were collected on a HORIBA Jobin Yvon SPEX Fluoromax-4 spectrafluorometer (90 °C angle geometry, 1 cm × 1 cm quartz cell). Before fluorescence analysis, the multiblock micellar stock solution was serially diluted with deionized water starting with a concentration of 0.41 mg/mL down to 6.3×10^{-7} mg/mL. Dynamic light scattering (DLS) data were acquired using a Malvern Zetasizer nanoZS instrument (Malvern Instruments, UK) at 25 °C using a scattering angle of 173°. Micellar solutions (concentrations ranging from 0.3 to 0.5 mg/mL in DI H_2O) were passed through a 0.22 μm PVDF filter prior to analysis, and measurements were made in triplicate. The data were analyzed by Malvern's DTS software (v. 6.01) using a cumulant analysis with a single-exponential fit. This analysis provided the hydrodynamic radius (D_h) of the particles as well as the polydispersity index (PDI). Bright field TEM imaging was performed on a FEI Tecnai 12 and JEOL JEM 2000FX microscope operating at an accelerating voltage of 120 and 200 kV, respectively. TEM samples were prepared by applying a drop of polymer solution (about 4 μL) onto a carbon-coated copper TEM grid (300 mesh) and allowing the solvent to evaporate under ambient conditions. Afterward, samples were stained with uranyl acetate or ruthenium tetroxide. A droplet of freshly prepared saturated uranyl acetate aqueous solution (about 10 μL) was deposited onto the dried samples. After about 1 min, the excess solution was wicked away by a piece of filter paper, and the sample was allowed to dry for TEM observation. Ruthenium tetroxide staining was applied via a vapor-staining method.[41]

Synthesis of 3-(1,1,1-Trimethylsilyl)-2-propynyl 2-Bromo-2-methylpropanoate. The synthesis was accomplished by following previously published methods described by Opsteen and van Hest.[42] A round-bottom flask was charged with 3-(trimethylsilyl) propargyl alcohol (1.2 mL, 7.8 mmol), triethylamine (1.6 mL, 11.5 mmol), and THF (50 mL). The colorless solution was cooled to 0 °C with an ice bath before adding dropwise a solution of 2-bromo-2-methylpropionyl bromide (1.4 mL, 11.5 mmol) in THF (25 mL). Upon complete addition, the ice bath was removed and the solution stirred at room temperature for 1 h. After this time, the precipitate was filtered, methanol (5 mL) was added to quench the remaining 2-bromo-2-methylpropionyl bromide, and the solution was concentrated by rotary

evaporation to a yellow oil. The crude product was purified by flash chromatography (SiO_2, 19:1 heptane−ethyl acetate) yielding the desired product as a clear oil (1.97 g, 91%). ^{1}H NMR ($CDCl_3$, δ): 4.76 (s, $-OCH_2-$), 1.95 (s, $-(CH_3)_2$), 0.18 (s, $-Si(CH_3)_3$).

Synthesis of α-TMS-alkynyl-poly(*tert*-butyl acrylate) (α-TMS-alkynyl-P*t*BA) (1). In a typical procedure, copper(I) bromide (0.260 g, 1.81 mmol), initiator 3-(1,1,1-trimethylsilyl)-2-propynyl 2-bromo-2-methylpropanoate (0.500 g, 1.81 mmol), *tert*-butyl acrylate (12.7 g, 99.1 mmol), PMDETA (0.320 g, 1.85 mmol), and toluene (6.00 mL) were added to a 150 mL round-bottom Schlenk vessel. The mixture was degassed by three freeze−pump−thaw cycles, backfilled with nitrogen, and placed in an oil bath at 80 °C. After 2.5 h, the polymerization was stopped by placing the vessel in an ice bath. The contents of the tube were diluted with THF, passed through a column of basic alumina, and precipitated three times into a 7:3 mixture of methanol/water (200 mL in total). The solution was decanted yielding the viscous polymer which was subsequently dried and analyzed by ^{1}H NMR and SEC (6.2 g, 49% yield). ^{1}H NMR ($CDCl_3$, δ): 4.64 (m, $-CH_2O-$), 2.22 (m, $-CH_2CH-$), 1.84, 1.53 (m, $-CH_2CH-$), 1.44 (s, $-C(CH_3)_3-$), 1.16 (m, $-CH_3-$), 0.16 ($-Si(CH_3)_3$).

Synthesis of α-TMS-alkynyl-poly(*tert*-butyl acrylate-*b*-styrene) (α-TMS-alkynyl- P*t*BA-PS) (2). In a typical procedure, polymer **1** (6.20 g, 0.918 mmol) was dissolved in styrene (9.57 g, 91.9 mmol) in a 150 mL round-bottom Schlenk vessel, and then copper(I) bromide (0.330 g, 2.30 mmol) and PMDETA (0.400 g, 2.30 mmol) were added to the flask. The mixture was degassed by three freeze−pump−thaw cycles, backfilled with nitrogen, and placed in an oil bath at 85 °C. After 1 h, the polymerization was stopped by placing the vessel in an ice bath. The contents of the tube were diluted with THF, passed through a column of basic alumina, and precipitated three times into methanol/water (200 mL, 7:3 methanol/water). The solution was decanted yielding the white polymer which was subsequently dried and analyzed by ^{1}H NMR and SEC (11.0 g, 65% yield). ^{1}H NMR ($CDCl_3$, δ): 7.08−6.45 (m, Ar−*H*), 4.65 (m, $-CH_2O-$), 2.22 (m, $-CH_2CH-$), 1.85 (m, $-CH_2CH-$), 1.52 (m, $-CH_2CH-$), 1.43 (s, $-C(CH_3)_3-$), 0.17 ($-Si(CH_3)_3$).

Synthesis of α-TMS-alkynyl-ω-azido-P*t*BA-PS (3). A 250 mL round-bottom flask was charged with polymer **2** (11.0 g, 0.560 mmol) which was subsequently dissolved in DMF (50 mL). Sodium azide (0.180 g, 2.77 mmol) was then added, and the orange solution was allowed to stir for 24 h. After this time, the polymer was precipitated three times by dissolution in THF followed by precipitation into cold methanol/water (200 mL, 7:3 methanol/water). The solution was decanted yielding the white polymer which was dried and analyzed by ^{1}H NMR and SEC (6.80 g, 62% yield). ^{1}H NMR ($CDCl_3$, δ): 7.08−6.45 (m, Ar−*H*), 4.65 (m, $-CH_2O-$), 2.22 (m, $-CH_2CH-$), 1.85 (m, $-CH_2CH-$), 1.52 (m, $-CH_2CH-$), 1.43 (s, $-C(CH_3)_3-$), 0.17 ($-Si(CH_3)_3$).

Synthesis of α-Alkynyl-ω-azido-P*t*BA-PS (4). Polymer **3** (6.79 g, 0.340 mmol) was dissolved in THF (50 mL) to form a yellow solution. TBAF (3.40 mL, 3.42 mmol) was then added, and the solution turned peach in color. The solution was allowed to stir overnight before being concentrated via rotary evaporation to a viscous oil. The polymer was diluted slightly with THF and precipitated three times into cold methanol/water (200 mL, 7:3 methanol/water). The polymer was dried and analyzed by ^{1}H NMR and SEC (1.04 g, 71% yield, 100% deprotection). ^{1}H NMR ($CDCl_3$, δ): 7.08−6.45 (m, Ar−*H*), 4.65 (m, $-CH_2O-$), 2.22 (m, $-CH_2CH-$), 1.85 (m, $-CH_2CH-$), 1.52 (m, $-CH_2CH-$), 1.43 (s, $-C(CH_3)_3-$).

Synthesis of P*t*BA-PS Multiblock Copolymers ((PtBA-PS)$_n$) (5). This was conducted by following a literature procedure by Tsarevsky et al.[43] Deprotected P*t*BA-PS-N_3 (**4**) (7.01 g, 0.491 mmol) was combined with copper(I) bromide (0.071 g, 0.491 mmol) and degassed by performing five vacuum−nitrogen cycles, leaving the flask under nitrogen. Purged DMF (30 mL) was then added, and the solution was allowed to stir at room temperature for 5 days. The viscous polymer solution was diluted with THF, passed through a column of alumina, and precipitated three times into methanol (200 mL). The polymer was dried under vacuum and analyzed by ^{1}H NMR and SEC (3.0 g, 43% yield). ^{1}H NMR ($CDCl_3$, δ): 7.08−6.45 (m, Ar−*H*), 2.16 (m, $-CH_2CH-$), 1.85 (m, $-CH_2CH-$), 1.60 (m, $-CH_2CH-$), 1.43 (s, $-C(CH_3)_3-$).

Synthesis of Poly(acrylic acid-*b*-styrene) Multiblock Copolymers ((PAA−PS)$_n$) (6). P*t*BA-PS multiblock **5** (3.02 g, 0.041 mmol) was dissolved in dichloromethane (8.5 mL) to form a yellow paste. Trifluoroacetic acid (5 mL, 65.3 mmol) was added to form a viscous, yellow solution. After 21 h, the material precipitated from the yellow solution to form a light brown gelatinous mass. The solution was decanted, and the pat of material was dissolved in DMF (∼10−15 mL). The solution was transferred into presoaked dialysis tubing (MWCO = 1000), dialyzed against deionized water for 2 days (1 L of deionized water changed twice daily), and lyophilized to recover the PAA−PS multiblock as a white powder (1.66 g, 55% yield). ^{1}H NMR (*d*-DMSO, δ): 7.05−6.50 (m, Ar−*H*), 2.20 (m, $-CH_2CH-$), 1.76 (m, $-CH_2CH-$), 1.49−1.34 (m, $-CH_2CH-$).

Self-Assembly of PAA−PS Multiblocks. A small amount of multiblock (∼10 mg) was dissolved in THF (∼10 mL) at a concentration of 1 mg/mL. The solution was transferred into presoaked dialysis tubing (MWCO = 1000) and extensively dialyzed against deionized water (1 L, water was changed twice daily) for 3−4 days.

Critical Micelle Concentration Determination. A stock solution of pyrene was made by dissolving pyrene (5 mg, 25 μmol) in acetone (1 L) to form a 2.5×10^{-5} M solution. The pyrene solution (24 μL) was dropped into empty vials, and the acetone was evaporated overnight in a vacuum oven. The PAA−PS multiblock micellar stock solution was serially diluted with deionized water starting with a concentration of 0.41 mg/mL down to 6.3×10^{-7} mg/mL. Each polymer solution (1 mL) was transferred to a vial containing pyrene and stirred overnight. The final pyrene concentration in the polymer solutions reached 6×10^{-7} M (which is less than the pyrene saturation concentration in water).[44] Fluorescence determinations were made by exciting samples at 333 nm, using a 3 nm slit width for excitation and a 1.5 nm slit width for emission. Emission wavelengths were scanned from 350 to 500 nm. The intensities of the I_1 (372 nm) to I_3 (383 nm) vibronic bands were evaluated for each sample, and the ratio of these were plotted against the log of the concentration of each polymeric sample.[45] The critical micelle concentration (cmc) was taken as the intersection of two regression lines calculated from the linear portions of the graphs.

■ RESULTS AND DISCUSSION

Synthesis of PAA−PS Multiblock Copolymers. Although much work has been devoted toward the synthesis and characterization of PAA−PS diblock copolymers,[46] there has not been any report on the synthesis of PAA−PS multiblock copolymers, despite the potential useful applications of such molecules in the assembly of various nanostructures. In these studies, PAA was selected as the corona-forming block due to its water solubility and high degree of functionality for later attachment of biomolecules. PS was chosen as the core-forming block because of its high glass transition temperature (∼100 °C) which helps to stabilize the micelle after formation.[40] Here, we present our synthetic strategy toward the synthesis of high molecular weight PAA−PS multiblocks.

A protected alkyne initiator 3-(1,1,1-trimethylsilyl)-2-propynyl 2-bromo-2-methylpropanoate was used for the ATRP of *tert*-butyl acrylate (*t*BA) to form α-TMS-alkynyl-poly(*tert*-butyl acrylate) (α-TMS-alkynyl-P*t*BA, **1**, Scheme 1).[42,47,48] The

TMS-protected initiator was employed in order to avoid copper complexation with the terminal alkyne as well as radical addition to the alkyne during polymerization.[42,49] The α-TMS-alkynyl-P*t*BA macroinitiator was chain extended with styrene to form the diblock copolymer α-TMS-alkynyl-P*t*BA-*b*-PS (**2**, Scheme 1). The SEC analysis of the homopolymer to diblock copolymer transition shows a shift to higher molecular weight with no apparent homopolymer **1** contamination of the diblock **2** (Figure 1). Nucleophilic displacement of the terminal bromine atom with sodium azide provided the azide end-terminal polymer (α-TMS-alkynyl-ω-azido-P*t*BA-*b*-PS, **3**, Scheme 1), and subsequent quantitative removal (with TBAF) of the TMS protecting group from the alkyne, as observed by the complete disappearance of the TMS methyl group protons in the ^{1}H NMR spectrum (Figure S1, Supporting Information), afforded the desired α,ω-heterotelechelic P*t*BA-*b*-PS diblock copolymer (**4**, Scheme 1 and Table 1).[42,43,50] With the α-alkynyl, ω-azido-P*t*BA-PS in hand, copper-catalyzed alkyne-azide cycloaddition (CuAAC) was performed in order to couple the chains together to form the P*t*BA-PS multiblock copolymer (**5**, Scheme 1 and Table 1), and the reaction was directly analyzed via SEC (prior to deprotection) owing to the necessity for solubility in THF for analysis.[43] The diblock was self-coupled in the presence of CuBr, along with DMF, which served as a solvent and weakly coordinating ligand at room temperature.[51] The molecular weights of the P*t*BA-PS diblocks and the smallest and largest P*t*BA-PS multiblocks obtained from different synthetic batches are listed in Table 1. The M_n values of the multiblocks ranged from 43.8 to 73.3 kg/mol, while the M_w values ranged from 95.2 to 209 kg/mol, suggesting that up to nine diblocks were incorporated into the multiblocks. Although the total molecular weights and number of diblock repeats was observed to differ between different synthesized batches of the multiblock, the molar fraction of PS (assessed by ^{1}H NMR) remains similar when comparing two multiblock copolymers of different molecular weights. The molar fraction of PS in $(PtBA\text{-}PS)_9$ = 55 mol % and that of $(PtBA\text{-}PS)_4$ = 63 mol %. The batch-to-batch heterogeneity of the molecular weights of the multiblocks likely occurs due to small variations in reaction conditions during the step-growth process as well as due to small end-group functionality differences of the diblocks employed in the various multiblock syntheses. Nevertheless, as detailed below, the synthetic protocols permit the formation of well-defined nanoparticles at low critical micelle concentration values. Thus, the multiblock synthetic pathway, although complicated by heterogeneity, can still yield useful assembled structures (vide infra).

After formation of the multiblock, the *tert*-butyl groups of the P*t*BA block were deprotected with TFA to form the PAA−PS multiblock (**6**, Scheme 1).[52,53] The complete deprotection of the P*t*BA block was indicated by the disappearance of the *tert*-butyl group protons at 1.43 ppm in the ^{1}H NMR spectrum (Figure S2, Supporting Information) and the disappearance of the quaternary carbon atom at 80 ppm in the ^{13}C spectrum (data not shown), along with the shift of the carbonyl stretch in the ATR-IR spectrum from 1730 to 1720 cm^{-1} (Figure 2). In order to ensure that the multiblock backbone esters resulting from initiator **1** were not cleaved during the TFA deprotection of the *tert*-butyl esters, a sample of a PAA−PS multiblock was methylated with trimethylsilyldiazomethane[54] to form a poly(methyl acrylate-*b*-styrene) (PMA−PS) multiblock copolymer

Scheme 1. Synthetic Pathway for the Construction of Poly(acrylic acid-*b*-styrene) Multiblock Copolymers

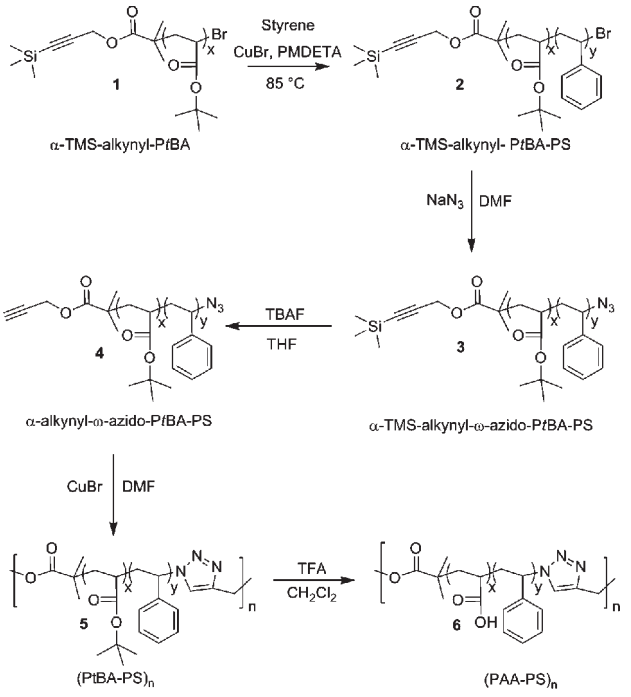

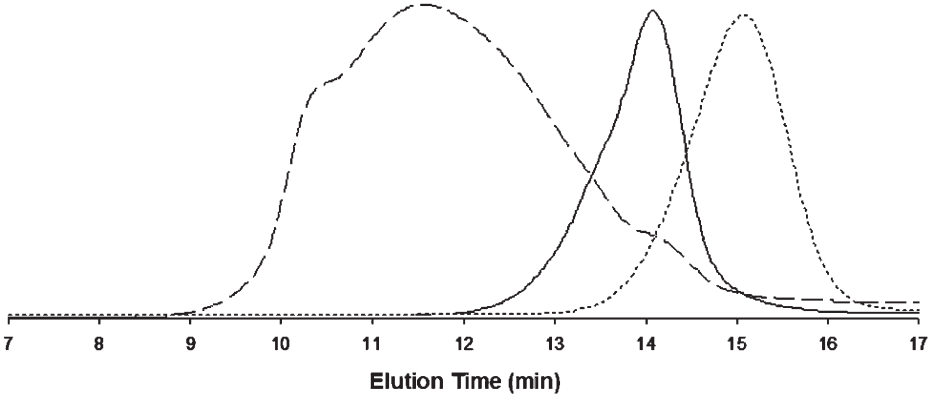

Figure 1. SEC traces of starting P*t*BA homopolymer (---) (M_n = 7.2 kg/mol, M_w/M_n = 1.27), diblock (—) (M_n = 18.3 kg/mol, M_w/M_n = 1.30), and multiblock $(PtBA\text{−}PS)_9$ after azide-alkyne cycloaddition (− − −) (M_n = 73.3 kg/mol, M_w = 209 kg/mol, M_w/M_n = 2.90).

dx.doi.org/10.1021/ma102869y |*Macromolecules* 2011, 44, 1942–1951

Table 1. Molecular Weight Data for the P*t*BA−PS Diblock and Multiblock Copolymers

	P*t*BA−PS, **4**			(P*t*BA−PS)$_n$, **5**			
ID	$M_{n,(SEC)}$[a] (kg mol^{-1})	$M_{w,(SEC)}$[a] (kg mol^{-1})	M_w/M_n	$M_{n,(SEC)}$[a] (kg mol^{-1})	$M_{w,(SEC)}$[a] (kg mol^{-1})	M_w/M_n	diblock repeats[b]
(P*t*BA−PS)$_9$	18.3	23.7	1.30	73.3	209	2.90	4−9
(P*t*BA−PS)$_4$	18.6	22.2	1.20	43.8	95.2	2.20	2−4

[a] Determined by SEC against polystyrene standards. [b] Calculated by ratio of $M_{n,SEC,(PtBA-PS)n}/M_{n,SEC,PtBA-PS}$ and $M_{w,SEC,(PtBA-PS)n}/M_{w,SEC,PtBA-PS}$.

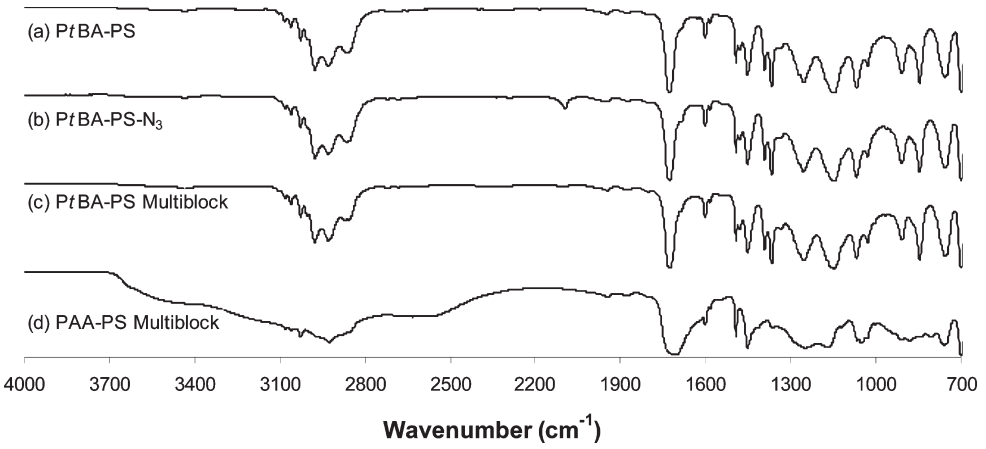

Figure 2. Representative ATR-IR spectra of a P*t*BA−PS diblock before (a) and after azidation (b), after click cycloaddition to form the P*t*BA−PS multiblock (c), and after hydrolysis of *tert*-butyl groups to form the PAA−PS multiblock (d).

and analyzed by SEC. The molecular weight of the PMA−PS multiblock (M_n = 29.8 kg/mol, M_w = 46.0 kg/mol) was slightly less than that of the parent P*t*BA-PS multiblock (M_n = 30.7 kg/mol, M_w = 50.4 kg/mol), which likely results from the loss of mass when the *tert*-butyl group is replaced by the methyl group (Figure S3, Supporting Information).[55] The good correlation of the polymer molecular weights before and after deprotection suggests that the backbone ester bonds were not cleaved by the TFA deprotection step. An additional experiment also confirmed that hydrolysis of the backbone esters was not occurring under TFA treatment. A polystyrene "multiblock" was synthesized from the CuAAC coupling of α-alkynyl-ω-azido-polystyrene chains and subjected to the same TFA treatment as the P*t*BA-PS multiblock copolymers. SEC analysis of the molecular weights of the PS "multiblock" before and after TFA treatment revealed that after treatment the molecular weight slightly increased, likely due to fractionation of smaller chains and shows that hydrolysis of the backbone did not occur ($M_{n,before}$ = 26.9 kg/mol; $M_{w,before}$ = 43.5 kg/mol; M_w/M_n = 1.62; $M_{n,after}$ = 34.8 kg/mol kg/mol; $M_{w,after}$ = 49.6 kg/mol; M_w/M_n = 1.43).

Multiblock Characterization Details. The growth of the α-TMS-alkynyl-P*t*BA homopolymer to the α-TMS-alkynyl-ω-azido-P*t*BA-*b*-PS diblock copolymer and subsequently to the (P*t*BA−PS)$_9$ multiblock copolymer was confirmed by SEC (Figure 1); results shown are representative of those observed for multiple syntheses of the multiblock copolymers. The α-TMS-alkynyl-P*t*BA homopolymer (M_n = 7.2 kg/mol, M_w/M_n = 1.27) had a unimodal distribution and the highest retention time, and the shift to the α-TMS-alkynyl-ω-azido-P*t*BA-*b*-PS diblock was observed at a lower retention time, showing an increase in the molecular weight and formation of the diblock (M_n = 18.3 kg/mol, M_w/M_n = 1.30). There is a slight high molecular weight shoulder in the trace of the diblock which likely results from bimolecular termination reactions. Even though this would potentially lead to the loss of bromine end groups, this event did not prohibit the formation of the multiblock copolymers. The P*t*BA−PS multiblock (M_n = 73.3 kg/mol, M_w/M_n = 2.85) showed a large shift to a molecular weight higher than the diblock copolymer and a broad molecular weight distribution, typical to that of polymers grown by step growth polymerization.[16,43] As mentioned above, the multiblocks contained up to nine repeats of the diblock copolymer based on SEC estimation (Table 1). The molecular weights of the diblock and multiblock copolymers were calculated by SEC using polystyrene standards. Therefore, the molecular weights and diblock copolymer repeats calculated are not absolute. The multiblocks generally had a low molecular weight shoulder with a similar retention time as the diblock copolymers (Figure 1). This may result from unreacted diblock copolymer or the formation of cyclic polymers and represented ∼5% of the material as calculated by integration of the multiblock SEC trace.[43,56] The high molecular weight shoulder seen in the multiblock trace of Figure 1 likely results from a high molecular weight multiblock which is apparent in the SEC trace due to the inherent heterogeneity of the multiblock; the breadth of the multiblock copolymer molecular weight distributions is consistent with that expected based on the condensation and step-growth nature of the multiblock polymerization. The P*t*BA-PS multiblocks were purified by precipitation before SEC analysis, and no further attempts to fractionate the polydisperse material were made.

The multiblock copolymers were also evaluated by ATR-IR spectroscopy. The installation of the azide group was easily observed by the appearance of the N═N═N antisymmetric stretch around 2090 cm^{-1} upon the conversion of P*t*BA−PS (Figure 2a) to P*t*BA-PS-N$_3$ (Figure 2b).[57−59] After coupling the diblock chains together to form the multiblock copolymer, the

Table 2. Dynamic Light Scattering and TEM Data for PAA−PS Multiblocks

ID[a]	$M_{n,(SEC)}$[b] (kg mol^{-1})	diblock repeats	$D_{h,DLS}$[c] (nm)	PDI[d]	$D_{ave,TEM}$[e] (nm)
$(PAA-PS)_9$	73.3	4−9	11	0.35	14 ± 2
$(PAA-PS)_4$	43.8	2−4	34	0.16	20 ± 4

[a] $(PAA-PS)_9$ concentration = 0.41 mg/mL; $(PAA-PS)_4$ concentration = 0.31 mg/mL. [b] $M_{n,SEC}$ is for the $(PtBA-PS)_n$ before deprotection and is determined by SEC against polystyrene standards. [c] *Z*-average hydrodynamic diameters of PAA−PS multiblock micelles in aqueous solution. [d] Polydispersity index for the micelle solution from DLS measurements. [e] TEM average diameter of micelles based on the analysis of 100 particles across four micrographs.

intensity of the azide stretch significantly decreased, corroborating formation of the P*t*BA−PS multiblock copolymer (Figure 2c). Because of overlap with other peaks of the polymer, the triazole N═N stretch was not apparent at 1465 cm^{-1}.[60] After deprotection of the *tert*-butyl groups from the P*t*BA−PS multiblock to form the PAA−PS multiblock, the presence of the carboxylic −OH stretch was obvious as a broad peak from ∼3600 to 2500 cm^{-1} (Figure 2d). Additionally, the carbonyl stretch shifted from 1730 cm^{-1} in traces a−c to 1720 cm^{-1} in trace d, indicative of complete hydrolysis of the *tert*-butyl groups.[55,61,62] The broadening of the carbonyl stretch found in trace d is likely due to the presence of both free carboxylic acid groups and intrapolymer hydrogen-bonded groups.[63−66]

PAA-PS Multiblock Assembly and Characterization. Via a solvent exchange process, the PAA−PS multiblocks were assembled by dissolution in THF followed by extensive dialysis against deionized water.[10] The critical micelle concentration (cmc) is the concentration at which unimeric block copolymers associate to form micelles in aqueous solution[67] and is an important value when considering the biological applications of a specific polymer system. Since micelles are thermodynamically stable above the cmc, it is of paramount importance that the cmc of the polymeric system be low enough to prevent immediate dissolution of the micelles to unimers upon intravenous injection.[40]

The cmc of an aqueous solution of self-assembled multiblock $(PAA-PS)_9$ (Table 2) was ascertained by steady-state fluorescence spectroscopy with pyrene used as a fluorescent probe. The ratio between the first and third highest energy vibrational bands (I_1/I_3) of pyrene has been correlated with solvent polarity.[45,68] Below the cmc of the polymer chains, assemblies are not present, and the I_1/I_3 ratio is equivalent to that of pyrene in water (∼1.6−1.8).[68] However, once assemblies are present, pyrene partitions into the hydrophobic core, and the I_1/I_3 ratio decreases. Representative data from these experiments are presented in Figure 3; the cmc value is determined from the intersection of the two linear regions of the plot. On the basis of replicate measurements, the cmc for multiblock $(PAA-PS)_9$ was found to be 2.0×10^{-4} mg/mL, lower than cmcs reported for other polymeric systems and suggesting the likely stability of the multiblock assemblies in solution. The cmc for multiblock $(PAA-PS)_4$ was also very low at 2.1×10^{-4} mg/mL. The total blood volume for an average individual is ∼5 L.[40] With a cmc of 2.0×10^{-4} mg/mL, a dose as low as the micelle solution concentration equivalent to 1 mg of $(PAA-PS)_9$ could be administered intravenously before the micelles would dissociate.

To our knowledge, there is only one other report of the cmc for an alternating multiblock copolymer. Du et al. synthesized a PNIPAM−P*t*BA−PNIPAM multiblock with an M_n = 87.4 kg/mol and an average number of 3−4 block repeats which had a cmc of 1.4×10^{-2} mg/mL.[39] This cmc value is higher by 2

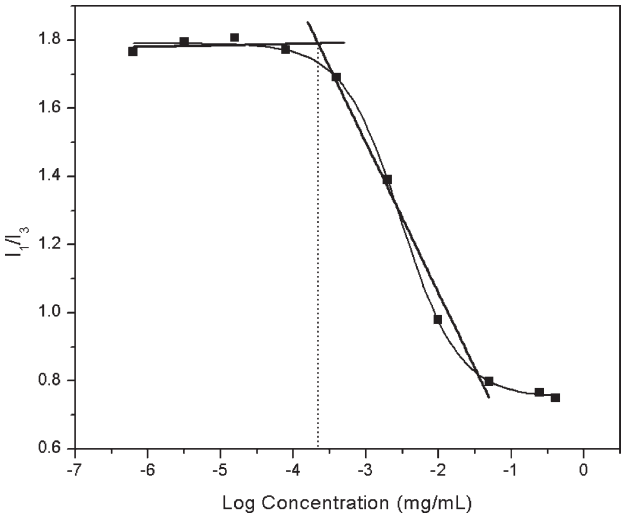

Figure 3. A representative plot of the I_1/I_3 values versus the logarithm of the concentration of $(PAA-PS)_9$.

orders of magnitude than the $(PAA-PS)_9$ multiblock presented here. Our cmc value of 2.0×10^{-4} mg/mL is also an order of magnitude lower than other diblock systems such as a poly(ethylene glycol-*b*-DL-lactide) ($PEG_{61}-PLA_{78}$) diblock with a cmc of 2.5×10^{-3} mg/mL,[69] a poly(ethylene oxide-*b*-styrene) ($PEO_{398}-PS_{108}$) diblock with a cmc of 1.0×10^{-3} mg/mL,[70] and a poly(acrylic acid-*g*-ethylene glycol diacrylate-*b*-*n*-butyl acrylate) (PAA_{80}-*g*-$PAA(HEA)_{20}$-*b*-$PnBA_{16}$) diblock with a cmc of 5.0×10^{-3} mg/mL.[10] Triblock copolymers of $PEO_{102}PS_{39}PEO_{102}$ had a cmc of 2×10^{-3} mg/mL,[70] and a system consisting of $PEO_{100}PPO_{65}PEO_{100}$ had a cmc of 1.1×10^{-2} mg/mL at 37 °C.[71] Eisenberg showed that increasing the hydrophobic PS block length in poly(styrene-*b*-sodium acrylate) (PS−PANa) diblocks from 6 to 110 units decreased the cmc from 1.6×10^{-5} to 5×10^{-8} M, which is also greater than an estimated cmc of $(PAA-PS)_9$ of 2.7×10^{-9} M.[68] It is well-known that the cmc is greatly affected by the overall hydrophobic to hydrophilic balance within the polymer, with decreasing cmc values observed with an increase in the hydrophobic content of the polymer.[67] Given that the $(PAA-PS)_9$ is equipped with blocks of similar relative lengths as those in the systems described above (∼56 units of PAA per 107 units of PS in each diblock repeat of $(PAA-PS)_9$), we postulate that our PAA−PS multiblock copolymer cmc values are likely lower than other similar diblock and triblock systems because of the high local concentration of hydrophobic to hydrophilic polymer blocks which allows assembly at a lower concentration than would otherwise be possible.

Dynamic light scattering (DLS) studies were conducted to characterize the PAA−PS multiblock structures formed in water. PAA−PS multiblocks were dissolved in THF at a concentration

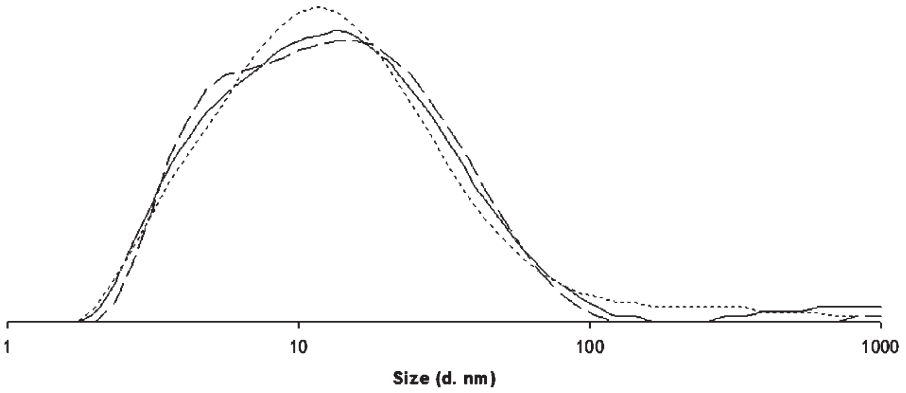

Figure 4. DLS data for the intensity-based *z*-average hydrodynamic diameter of the $(PAA-PS)_9$ assemblies in deionized water.

of 1 mg/mL and dialyzed extensively against deionized water for several days to form the assembled structures in aqueous solution. Multiblock $(PAA-PS)_9$ assembled on the nanometer scale forming structures ~11 nm (Table 2). Assemblies from smaller multiblocks (containing 2−4 blocks) formed larger particles (*z*-average diameter ~35 nm) than $(PAA-PS)_9$ (Figure S4, Supporting Information). As shown in Figure 4, the $(PAA-PS)_9$ particles were unimodal in diameter, but the distribution of diameter sizes was fairly broad. The polydispersity index of $(PAA-PS)_9$ was 0.35 (relative standard deviation of 59% with a PDI width of ±6.3 nm). Assemblies from multiblock samples, when analyzed after 2 months, showed no large increase in aggregate size, suggesting that the assemblies are reasonably stable in aqueous solution over this time frame.

Our data indicate that multiblocks of greater molecular weight form particles of smaller hydrodynamic diameter, which may result from the intramolecular collapse of the longer multiblock chain which would result in small particles. Zhou et al. showed that in multiblock copolymers of $(PDMA_{42}-PNIPAM_{37})_n$ and $(PDMA_{105}-PNIPAM_{106})_n$, which both contain 6−7 block repeats, the structures change from larger multimolecular micelles for the shorter multiblock to small unimolecular micelles for the longer multiblock, upon collapse of the insoluble PNIPAM chains at elevated temperatures.[13]

Additionally, the larger molar ratio of PS to PAA in $(PAA-PS)_4$ (63 mol % PS) compared with $(PAA-PS)_9$ (55 mol %) would also cause the interface between PS and PAA to be of lower curvature within the particle. This smaller interfacial curvature between PAA and PS blocks would help produce larger overall particle sizes with less curvature between PAA domains and PS domains with $(PAA-PS)_4$.[72] Another possibility for the decrease in size of the nanoparticles formed from the $(PAA-PS)_9$ is an increase in multiblock polydispersity (from $(PAA-PS)_4$ (M_w/M_n = 2.17) to $(PAA-PS)_9$ (M_w/M_n = 2.85). Terreau et al. showed that increasing the polydispersity of the PAA block of a variety of PAA−PS diblock copolymers caused a decrease in the size of assembled vesicles to a point where spheres and vesicles coexisted.[73] For example, PAA−PS chains with a PDI of 1.10 had a vesicle size of 270 nm, and after increasing the PDI to 2.13, the vesicles decreased in size to 85 nm. They postulated that shorter PAA−PS chains aggregate to the inside of the vesicle, allowing for a smaller vesicle interior, while the longer chains segregate to the exterior corona. At some point, the interactions between partially charged PAA chains are unfavorable and spheres would form.

There are very few reports in the literature reporting the formation of small particles by multiblock copolymers. Hadjiantoniou et al. showed by DLS that low molecular weight multiblocks containing M_n values <23 kg/mol and 2−3 blocks of poly[(2-dimethylamino)ethyl methacrylate-*b*-methyl methacrylate] form flowerlike micelles with diameters <23 nm, but no TEM data were shown to support their DLS results.[18,19] Du et al. synthesized a PNIPAM−P*t*BA−PNIPAM multiblock with an M_n = 87.4 kg/mol and an average number of 3−4 block repeats.[39] Even though small micelles were present in their TEM images, obvious large aggregates (>200 nm) were also present. Their DLS results showed that the micelles had an average diameter >167 nm. Despite the moderately broad assembly polydispersities, these $(PAA-PS)_n$ multiblocks are still unique in that they assemble into discrete particles less than 35 nm as observed by DLS and as corroborated by TEM data (vide infra).

Transmission electron microscopy (TEM) was also employed to characterize the assembled structures of the PAA−PS multiblocks. An aqueous solution of assembled multiblock $(PAA-PS)_9$ = 0.41 mg/mL was subjected to TEM analysis after staining with uranyl acetate (Figure 5).[74] In this case, the uranyl acetate serves as both a negative stain surrounding the particles and a positive stain for PAA within the particles due to interaction with the slightly charged PAA blocks.[1] As seen in Figure 5, $(PAA-PS)_9$ produced spherical assemblies with an average diameter of 14 nm, which corroborates the DLS data (D_h = 11 nm). Although TEM provides a local characterization method, the distribution of particle sizes in the TEM images is also consistent with the DLS results above. Since the original P*t*BA−PS multiblocks were not fractionated to reduce the polydispersity, we were initially surprised to find such uniform spherical structures after assembly. However, as mentioned above, Terreau et al. have shown that increasing the polydispersity of the PAA block in a PAA−PS diblock system decreased the size and polydispersity of the vesicles formed, suggesting that the polydispersity of our multiblock system may not be detrimental.[73] The particles appear as overall lighter spheres against a dark background resulting from the uranyl acetate negative staining. Darkened regions are also apparent within the boundary of the spheres, most easily seen in Figure 5B,C, suggesting the potential inclusion of PAA chains within the assembled structure and the production of multicompartments within the particles. Ruthenium tetroxide staining of the PS blocks darkened the spherical assemblies uniformly (Figure S5, Supporting Information), suggesting that the PS domains are dispersed throughout the nanoparticles; further

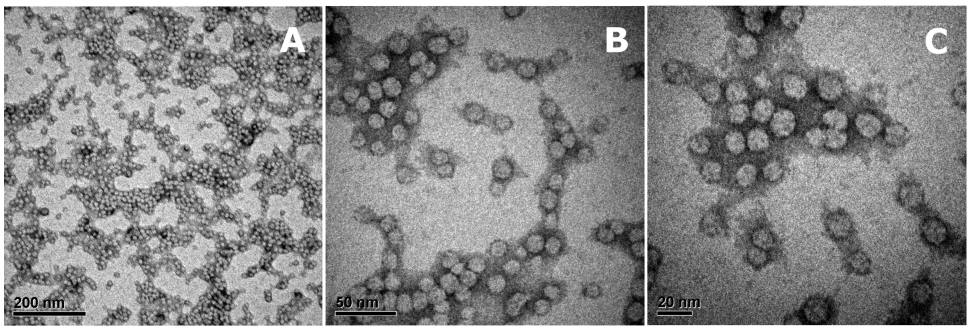

Figure 5. TEM morphologies for $(PAA-PS)_9$ at 0.41 mg/mL with (A) 200 nm scale bar, (B) 50 nm scale bar, and (C) 20 nm scale bar. The samples were stained with uranyl acetate before imaging.

characterization will permit elucidation regarding the nanoscale intraparticle organization of the PAA and PS blocks.

One of the more uniform multiblock assemblies observed by TEM was seen by Sommerdijk et al., who observed vesicles with diameters of 100−180 nm for poly(methylphenylsilane)-*alt*-PEO $(PMPS-PEO)_n$ multiblock copolymers with an M_n = 27 kg/mol and an average of 2.5 block repeats.[22] They proposed that the rigid PMPS segments were arranged in a parallel fashion, flanked by the hydrophilic PEO segments in order to form the vesicles. Multiblock copolymers of $(PS-PEO)_n$ with molecular weights from M_n = 19.6−99.6 kg/mol and an average of four block repeats resulted in a range of morphologies when the polystyrene block was increased in molecular weight relative to a constant weight for the PEO block.[12] The morphologies consisted of large aggregates, such as leaflike aggregates ranging from 1 to 1.5 μm in diameter and lamellar aggregates on the order of 500−700 nm. The most uniform particles consisted of vesicles that were 40−60 nm in diameter which coexisted with larger starlike vesicles.[12] Multiblocks of $(PNIPAM\text{-}PtBA)_n$ with an M_n = 87.4 kg/mol and an average number of 3−4 block repeats showed a range of structures by TEM as the concentration of polymer increased in solution.[39] As the polymer concentration increased from 0.025 up to 0.25 wt %, toroid structures, then cagelike structures followed by small micelles coexisting with their larger aggregates were present.

It is obvious that there are numerous variables which control the morphologies formed from the assembly of multiblock copolymers (just as there are for di- and triblock copolymers): molecular weight of the blocks, total number of blocks, relative block lengths of the hydrophobic to hydrophilic blocks, polydispersity of the blocks, polymer concentration, solvents, water content, and so forth.[38] This complexity makes it difficult to compare one polymer system to the next. However, this report details the first synthesis of $(PtBA-PS)_n$ multiblocks and the corresponding deprotected amphiphilic $(PAA-PS)_n$ multiblocks. The $(PAA-PS)_n$ multiblocks presented here represent the first report of uniform and discrete particles <35 nm in diameter, as confirmed by both DLS and TEM, assembled from a multiblock copolymer. This system has an advantage over other multiblock systems discussed earlier in that the hydrophilic PAA block has functionality which will provide ample opportunity for the future conjugation of biomolecules for drug delivery. These results offer various future directions from which to expand current knowledge regarding assembly, biomolecule attachment, and subsequent drug delivery. Future work will include studying the morphological transitions of this polymer system with regard to solvent and water content. The relative block sizes of the polymers, along with overall size of the polymer system will be altered in order to deduce the effects on the cmc and assembly. The $(PAA-PS)_n$ should also be responsive to pH changes, providing an additional trigger for self-assembly.

CONCLUSIONS

We have employed an alkyne-containing ATRP initiator to synthesize heterotelechelic poly(*tert*-butyl acrylate-*b*-styrene) containing an α-alkyne moiety and an ω-azide group. The growth of the polymers was controlled, with the homo- and diblock polymers displaying narrow molecular weight distributions. Multiblock copolymers were synthesized by the copper-catalyzed azide−alkyne cycloaddition of azide−alkyne end functional poly(*tert*-butyl acrylate-*b*-styrene) diblock copolymers. The P*t*BA−PS multiblock copolymers were deprotected to form PAA−PS multiblocks which were assembled to form nanostructures <35 nm in diameter as observed by DLS. TEM images confirmed the formation of spherical particles which were monodisperse in distribution, and staining of the nanoparticles confirmed the presence of PAA; these particles may thus be useful for the attachment and delivery of relevant biomolecules.

ASSOCIATED CONTENT

Supporting Information. Figures of ^{1}H NMR spectra of P*t*BA-PS diblock, P*t*BA-PS multiblock, and PAA−PS multiblock, SEC traces of the methylation of PAA−PS multiblock to PMA−PS, DLS and TEM data for $(PAA-PS)_4$, along with TEM images of $(PAA-PS)_9$ stained with ruthenium tetroxide. This material is available free of charge via the Internet at http://pubs.acs.org.

AUTHOR INFORMATION

Corresponding Authors

*X.J.: Ph 302-831-6553, Fax 302-831-4545, e-mail xjia@udel.edu. K.L.K.: Ph 302-831-0201, Fax 302-831-4545, e-mail kiick@udel.edu.

ACKNOWLEDGMENT

The authors thank Dr. Carl Giller for FT-IR assistance. NMR spectra were obtained with instrumentation supported by NSF CRIF: MU, CHE 0840401. The authors also thank the National Science Foundation (DMR 0239744, DMR 0907478, and DMR 0906815) and the University of Delaware Faculty Startup Funds for financial support. The project described was also supported in part by the National Institutes of Health (2P20RR017716, from

the National Center for Research Resources (NCRR), a component of the National Institutes of Health); the contents of this manuscript are solely the responsibility of the authors and do not necessarily represent the official views of NCRR or NIH. The W. M. Keck electron microscopy lab in the College of Engineering at the University of Delaware is acknowledged along with Dr. Chao-ying Ni and Mr. Frank Kriss for their EM lab assistance.

REFERENCES

(1) Cui, H.; Chen, Z.; Zhong, S.; Wooley, K. L.; Pochan, D. J. *Science* **2007**, *317*, 647–647.
(2) Matsen, M. W.; Bates, F. S. *J. Chem. Phys.* **1997**, *106*, 2436–2448.
(3) Zupancich, J. A.; Bates, F. S.; Hillmyer, M. A. *Biomacromolecules* **2009**, *10*, 1554–1563.
(4) Li, Z.; Hillmyer, M. A.; Lodge, T. P. *Nano Lett.* **2006**, *6*, 1245–1249.
(5) Schacher, F.; Walther, A.; Mu ller, A. H. E. *Langmuir* **2009**, *25*, 10962–10969.
(6) Fang, B.; Walther, A.; Wolf, A.; Xu, Y.; Yuan, J.; Müller, A. H. E. *Angew. Chem., Int. Ed.* **2009**, *48*, 2877–2880.
(7) Zheng, R.; Liu, G.; Yan, X. *J. Am. Chem. Soc.* **2005**, *127*, 15358–15359.
(8) Tang, C.; Lennon, E. M.; Fredrickson, G. H.; Kramer, E. J.; Hawker, C. J. *Science* **2008**, *322*, 429–429.
(9) Sun, G.; Fang, H.; Cheng, C.; Lu, P.; Zhang, K.; Walker, A. V.; Taylor, J. S.; Wooley, K. L. *ACS Nano* **2009**, *3*, 673–673.
(10) Xiao, L.; Liu, C.; Zhu, J.; Pochan, D. J.; Jia, X. *Soft Matter* **2010**, *6*, 5293–5297.
(11) Halperin, A. *Macromolecules* **1991**, *24*, 1418–1419.
(12) Jia, Z.; Xu, X.; Fu, Q.; Huang, J. *J. Polym. Sci., Part A: Polym. Chem.* **2006**, *44*, 6071–6082.
(13) Zhou, Y.; Jiang, K.; Song, Q.; Liu, S. *Langmuir* **2007**, *23*, 13076–13084.
(14) Dadmun, M. *Macromolecules* **1996**, *29*, 3868–3874.
(15) Eastwood, E. A.; Dadmun, M. D. *Macromolecules* **2002**, *35*, 5069–5077.
(16) Grieshaber, S. E.; Farran, A. J. E.; Lin-Gibson, S.; Kiick, K. L.; Jia, X. *Macromolecules* **2009**, *42*, 2532–2532.
(17) Ryu, C. Y.; Ruokolainen, J.; Fredrickson, G. H.; Kramer, E. J.; Hahn, S. F. *Macromolecules* **2002**, *35*, 2157–2166.
(18) Hadjiantoniou, N. A.; Krasia-Christoforou, T.; Loizou, E.; Porcar, L.; Patrickios, C. S. *Macromolecules* **2010**, *43*, 2713–2720.
(19) Hadjiantoniou, N. A.; Triftaridou, A. I.; Kafouris, D.; Gradzielski, M.; Patrickios, C. S. *Macromolecules* **2009**, 9750–9754.
(20) Nagata, Y.; Masuda, J.; Noro, A.; Cho, D.; Takano, A.; Matsushita, Y. *Macromolecules* **2005**, *38*, 10220–10225.
(21) Cheng, J.; Khin, K. T.; Jensen, G. S.; Liu, A.; Davis, M. E. *Bioconjugate Chem.* **2003**, *14*, 1007–1017.
(22) Sommerdijk, N.; Holder, S. J.; Hiorns, R. C.; Jones, R. G.; Noltes, R. J. M. *Macromolecules* **2000**, *33*, 8289–8294.
(23) Bae, Y. H.; Huh, K. M.; Kim, Y.; Park, K. H. *J. Controlled Release* **2000**, *64*, 3–13.
(24) Lee, J. W.; Hua, F.; Lee, D. S. *J. Controlled Release* **2001**, *73*, 315–327.
(25) Lee, J.; Bae, Y. H.; Sohn, Y. S.; Jeong, B. *Biomacromolecules* **2006**, *7*, 1729–1734.
(26) Wu, C.; Xie, Z.; Zhang, G.; Zi, G.; Tu, Y.; Yang, Y.; Cai, P.; Nie, T. *Chem. Commun.* **2002**, 2898–2899.
(27) Wang, W. J.; Li, T.; Yu, T.; Zhu, F. M. *Macromolecules* **2008**, *41*, 9750–9754.
(28) Sahin, E.; Kiick, K. L. *Biomacromolecules* **2009**, *10*, 2646–2651.
(29) Zhang, Q.; Ye, J.; Lu, Y.; Nie, T.; Xie, D.; Song, Q.; Chen, H.; Zhang, G.; Tang, Y.; Wu, C. *Macromolecules* **2008**, *41*, 2228–2234.
(30) Chen, Y.; Guan, Z. *J. Am. Chem. Soc.* **2010**, *132*, 4577–4579.
(31) Liao, S. W.; Yu, T. B.; Guan, Z. *J. Am. Chem. Soc.* **2009**, *131*, 17638–17646.
(32) Higaki, Y.; Otsuka, H.; Endo, T.; Takahara, A. *Macromolecules* **2003**, *36*, 1494–1499.
(33) Higaki, Y.; Otsuka, H.; Takahara, A. *Polymer* **2003**, *44*, 7095–7101.
(34) Motokucho, S.; Sudo, A.; Sanda, F.; Endo, T. *Chem. Commun.* **2002**, 1946–1947.
(35) You, Y. Z.; Hong, C. Y.; Pan, C. Y. *Chem. Commun.* **2002**, 2800–2801.
(36) Zhang, L.; Wang, Q.; Lei, P.; Wang, X.; Wang, C.; Cai, L. *J. Polym. Sci., Part A: Polym. Chem.* **2007**, *45*, 2617–2623.
(37) Liu, Y.; Cavicchi, K. A. *Macromol. Chem. Phys.* **2009**, *210*, 1647–1653.
(38) Choucair, A.; Lavigueur, C.; Eisenberg, A. *Langmuir* **2004**, *20*, 3894–3900.
(39) Du, B.; Mei, A.; Yang, Y.; Zhang, Q.; Wang, Q.; Xu, J.; Fan, Z. *Polymer* **2010**, *51*, 3493–3502.
(40) Allen, C.; Maysinger, D.; Eisenberg, A. *Colloids Surf., B* **1999**, *16*, 3–27.
(41) Vitali, R.; Montani, E. *Polymer* **1980**, *21*, 1220–1222.
(42) Opsteen, J. A.; Hest, J. C. M. *Chem. Commun.* **2005**, 57–59.
(43) Tsarevsky, N. V.; Sumerlin, B. S.; Matyjaszewski, K. *Macromolecules* **2005**, *38*, 3558–3561.
(44) Wang, L.; Zeng, R.; Li, C.; Qiao, R. *Colloids Surf., B* **2009**, *74*, 284–292.
(45) Colombani, O.; Ruppel, M.; Schubert, F.; Zettl, H.; Pergushov, D. V.; Müller, A. H. E. *Macromolecules* **2007**, *40*, 4338–4350.
(46) Zhang, L.; Eisenberg, A. *J. Am. Chem. Soc.* **1996**, *118*, 3168–3181.
(47) Rengifo, H. R.; Chen, L.; Grigoras, C.; Ju, J.; Koberstein, J. T. *Langmuir* **2008**, *24*, 7450–7456.
(48) Urbani, C. N.; Lonsdale, D. E.; Bell, C. A.; Whittaker, M. R.; Monteiro, M. J. *J. Polym. Sci., Part A: Polym. Chem.* **2008**, *46*, 1533–1547.
(49) Sumerlin, B. S.; Tsarevsky, N. V.; Louche, G.; Lee, R. Y.; Matyjaszewski, K. *Macromolecules* **2005**, *38*, 7540–7545.
(50) Eugene, D. M.; Grayson, S. M. *Macromolecules* **2008**, *41*, 5082–5084.
(51) Pascual, S.; Coutin, B.; Tardi, M.; Polton, A.; Vairon, J. P. *Macromolecules* **1999**, *32*, 1432–1437.
(52) Ma, Q.; Wooley, K. L. *J. Polym. Sci., Part A: Polym. Chem.* **2000**, *38*, 4805–4820.
(53) Francis, R.; Lepoittevin, B.; Taton, D.; Gnanou, Y. *Macromolecules* **2002**, *35*, 9001–9008.
(54) Couvreur, L.; Lefay, C.; Belleney, J.; Charleux, B.; Guerret, O.; Magnet, S. *Macromolecules* **2003**, *36*, 8260–8267.
(55) Bernaerts, K. V.; Willet, N.; Van Camp, W.; Jérôme, R.; Du Prez, F. E. *Macromolecules* **2006**, *39*, 3760–3769.
(56) Laurent, B. A.; Grayson, S. M. *J. Am. Chem. Soc.* **2006**, *128*, 4238–4239.
(57) White, M. A.; Johnson, J. A.; Koberstein, J. T.; Turro, N. J. *J. Am. Chem. Soc.* **2006**, *128*, 11356–11357.
(58) O'Reilly, R. K.; Joralemon, M. J.; Hawker, C. J.; Wooley, K. L. *J. Polym. Sci., Part A: Polym. Chem.* **2006**, *44*, 5203–5217.
(59) Joralemon, M. J.; O'Reilly, R. K.; Hawker, C. J.; Wooley, K. L. *J. Am. Chem. Soc.* **2005**, *127*, 16892–16899.
(60) Jin, Y.; Zhu, J.; Zhang, Z.; Cheng, Z.; Zhang, W.; Zhu, X. *Eur. Polym. J.* **2008**, *44*, 1743–1751.
(61) Wang, G.; Tong, X.; Zhao, Y. *Macromolecules* **2004**, *37*, 8911–8917.
(62) Rzayev, J.; Hillmyer, M. A. *J. Am. Chem. Soc.* **2005**, *127*, 13373–13379.
(63) Bucholz, T. L.; Loo, Y. L. *Macromolecules* **2008**, *41*, 4069–4070.
(64) Kaczmarek, H.; Szalla, A. *J. Photochem. Photobiol., A* **2006**, *180*, 46–53.
(65) Motzer, H. R.; Painter, P. C.; Coleman, M. M. *Macromolecules* **2001**, *34*, 8390–8393.
(66) Yates, R. A.; Caldwell, J. D.; Perkins, E. G. *J. Am. Oil Chem. Soc.* **1997**, *74*, 289–292.

(67) Kabanov, A. V.; Batrakova, E. V.; Alakhov, V. Y. *J. Controlled Release* **2002**, *82*, 189–212.
(68) Astafieva, I.; Zhong, X. F.; Eisenberg, A. *Macromolecules* **1993**, *26*, 7339–7352.
(69) Yasugi, K.; Nagasaki, Y.; Kato, M.; Kataoka, K. *J. Controlled Release* **1999**, *62*, 89–100.
(70) Wilhelm, M.; Zhao, C. L.; Wang, Y.; Xu, R.; Winnik, M. A.; Mura, J. L.; Riess, G.; Croucher, M. D. *Macromolecules* **1991**, *24*, 1033–1040.
(71) Croy, S. R.; Kwon, G. S. *J. Controlled Release* **2004**, *95*, 161–171.
(72) Spontak, R. J.; Smith, S. D. *J. Polym. Sci., Part B: Polym. Phys.* **2001**, *39*, 947–955.
(73) Terreau, O.; Luo, L.; Eisenberg, A. *Langmuir* **2003**, *19*, 5601–5607.
(74) Schuch, H.; Klingler, J.; Rossmanith, P.; Frechen, T.; Gerst, M.; Feldthusen, J.; Muller, A. H. E. *Macromolecules* **2000**, *33*, 1734–1740.